

The effect of deformation on the precipitation behaviour of an AlMgSi alloy A HRTEM study

Katharina Teichmann¹, Calin D. Marioara², Ketill Olav Pedersen², Sverre
Gulbrandsen-Dahl^{1,3}, Michal Kolar¹, Sigmund J. Andersen² and Knut Marthinsen¹

¹Norwegian University of Science and Technology, Trondheim, Norway

²SINTEF Materials and Chemistry, Trondheim, Norway

³Raufoss Technology & Industrial Management, Raufoss, Norway

The effect of 10% pre-deformation on the precipitation behaviour of an AA6060 Al-Mg-Si alloy was investigated via Transmission Electron Microscopy (TEM) with respect to precipitate microstructure and precipitate types. It is shown that the precipitation behaviour changes significantly in the presence of dislocations. Regarding the microstructure parameters, it could be seen that the precipitates are coarser, fewer and produce a higher volume fraction as compared to the un-deformed condition. By determining the precipitate type, it was found that the precipitation sequence changes such that most precipitates forming in the pre-deformed material are of the post- β'' type.

Keywords: aluminium, deformation, precipitation behaviour, transmission electron microscopy

1. Introduction

The most common class of Al alloys for structural applications are Al-Mg-Si-(Cu) alloys due to their properties like high strength/weight ratio, good formability and weldability and a good corrosion resistance. The Al-Mg-Si-(Cu) alloys age-harden as the result of nucleation and growth of a high number density of nanometer-sized metastable precipitates in the Al matrix. They have needle/lath/rod/plate morphologies with longest directions parallel to $\langle 001 \rangle_{\text{Al}}$. Precipitate type, microstructure parameters and corresponding mechanical properties depend on the alloy composition and heat treatment. The commonly accepted precipitation sequence in Al-Mg-Si-alloys is:

Atomic clusters \rightarrow GP-zones $\rightarrow \beta'' \rightarrow \beta'$, U1, U2, B' $\rightarrow \beta$, Si [1, 2, 3]

U1, U2 and B' precipitates are also known as Type A, Type B and Type C, respectively [4]. Andersen, Marioara et al [5, 6, 7] have shown that all metastable precipitates in the Al-Mg-Si-(Cu) alloys are structurally related through a Si network which is hexagonal or near-hexagonal in projection. The hexagonal c-axis is generally parallel with the long dimension of a precipitate, for example the axis of a needle. Because the precipitates are highly coherent with Al in this $\langle 100 \rangle_{\text{Al}}$ direction, the network c-periodicity equals the Al matrix periodicity 0.405 nm, or is a multiple of it. In the hexagonal base-plane a projected 'sub-cell' (SC) may be defined, with a and b approximately equal to 0.4 nm. The Si network SC deviates most from a hexagonal SC in the case of the pre- β'' and β'' phases since atoms here are closer to Al fcc-matrix positions.

Many products made of age-hardening aluminium alloys are produced by extrusion followed by a forming operation, which involve a certain degree of plastic deformation. Therefore, during the subsequent heat treatment the precipitation takes place in a material deformed to various degrees, which then affects the precipitation behaviour. Even without forming, the extruded profiles have to be stretched to straighten out a certain degree of buckling and bending of the profiles, so also in this case precipitation takes place in a slightly deformed material. As the dislocations introduced upon deformation act as heterogeneous nucleation sites, they modify the precipitation kinetics and may alter the precipitation sequence. An acceleration of the precipitation kinetics was observed by Genevois et al. [8] for an AA2024 alloy. Deschamps et al. [9] reports on a change in the precipitation sequence in an Al-Zn-Mg alloy. At the dislocations, the stable phase is precipitated. Matsuda et al.

[10, 11] have shown in AlMg₂Si alloys that a string-like phase forms on dislocation lines in early stages of annealing, which seems to grow into an elongated type phase with 1.04 nm periodicity. Further aging causes Type C (B') precipitates to form in Si-rich alloys, and β' in Mg-rich alloys. Yassar et al. [12] investigated by TEM the precipitation of metastable phases in an AA6022 alloy during DSC experiments, which does not necessarily reflect isothermal precipitation behaviour. It is shown, that in the presence of dislocations the β'' -precipitates are not formed.

Studying deformed materials is therefore important for a better understanding of precipitation and hardness mechanisms and for optimisation of industrial processes. The present work is closely connected to a comprehensive investigation of the effect of deformation on the mechanical response of a selection of AlMgSi (AA6xxx) alloys (Kolar et al. [13,14]). Extruded and solution heat treated specimens have been pre-deformed to different strains in the range 0-10 % and subsequently/simultaneously aged for different times and different aging temperatures (artificial aging), and the final mechanical response evaluated through room temperature tensile testing. Motivated by results from this work, the main purpose of the present work has been to do a detailed investigation of how 10% plastic deformation affects microstructure and precipitate type in one of these alloys, as compared to the precipitation behaviour of undeformed material.

2. Experimental

For all experiments, the alloy AA6060 was used. Its composition is shown in Table 1.

Table 1. Composition of the investigated alloy, wt%

Alloy	Al	Mg	Si	Mn	Fe	Ti	Cu	Zn	Cr
AA6060	Bal	0,47	0,41	0,02	0,2	0,008	0,003	0,009	0,002

The material was initially machined into round tensile test samples with a gauge length of 6 mm. Two conditions were prepared for TEM investigations. For both conditions, the material was first solution heat treated in a salt bath at 545°C for 5 minutes, then water quenched. Within 30 minutes at room temperature (RT), some of the samples were plastically deformed to 10%, while the others were left undeformed. All samples were further annealed at 190°C for 300 minutes, thus creating one undeformed, and one pre-deformed condition. TEM specimens were prepared by first cutting in the transversal direction 1.5 mm long discs from the tensile test samples. These discs were then mechanically ground to thicknesses of around 100 μ m. To reach thicknesses suitable for electron transparency in TEM, the samples were further electropolished with a Tenupol-3 machine. The electrolyte consisted of 1/3 HNO₃ and 2/3 methanol. The electrolyte temperature was kept at around -28°C. Three microscopes were used for the investigations, JEOL JEM-2010, JEOL JEM-2010F and a Philips CM30 operated at 150 kV. The point resolution of the JEOL JEM-2010F microscope used for high-resolution imaging is 0.2 nm.

Precipitate counting and measurements of average needle-lengths and cross-sections were performed on TEM film negatives acquired with the Philips CM30 microscope in bright field mode. Details about this microstructure quantification method can be found elsewhere [1]. The JEOL JEM-2010F and the JEOL JEM-2010 microscopes were used in High Resolution mode (HRTEM) for precipitate crystal structure identification. The precipitate particles can be uniquely identified by diffraction or HRTEM along their main axis. Due to their orientation in the Al matrix all micrographs therefore are from a $\langle 001 \rangle$ Al zone.

3. Results and discussion

A general overview of the precipitate microstructure in the two analysed conditions is presented in Fig. 1 and Table 2. The precipitates formed during annealing in the pre-deformed material are clearly larger and have a significantly lower number density, as compared to the precipitates in the

un-deformed condition. Fig. 1 also shows that for the pre-deformed condition precipitation seems to be favoured along dislocations, consistent with the observation by Kolar et al. [14] that the artificial aging response is faster than in undeformed material. The defects serve on one hand as heterogeneous nucleation sites leading to a favourable and fast nucleation at the dislocation cores (see Fig. 1), and on the other hand they are fast diffusion paths for atoms leading to a faster coarsening of the precipitates which again result in coarser precipitates.

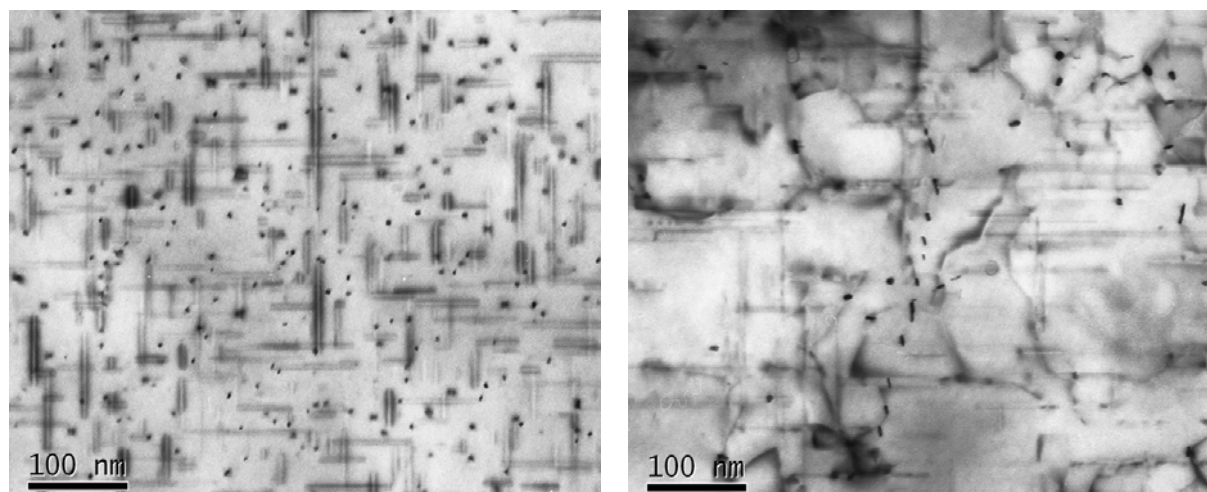


Fig. 1 Overview of the microstructure in AA6060 after 300 min heat treatment at 190°C a) without (0 %) pre-deformation and b) with 10% pre-deformation. Thicknesses of the imaged areas are 135 nm and 189.2 nm for the un-deformed and pre-deformed conditions, respectively.

Table 2. Microstructure parameters for 0% and 10% pre-deformed samples of AA6060 after annealing 300 min at 190°C.

Parameter	undeformed	10% pre-deformed
<I>	41.64 nm \pm 0.05nm	116.12 nm \pm 0.11 nm
<CS>	8.9 nm ² \pm 0.46 nm ²	26.66 nm ² \pm 0.48 nm ²
< ρ >	12675 needles/ μ m ³ \pm 0.15 needles/ μ m ³	2296 needles/ μ m ³ \pm 0.11 needles/ μ m ³
<VF>	0.470% \pm 0.47%	0.711% \pm 0.5%

The types of precipitates in the undeformed and the pre-deformed materials were determined by HRTEM. This was done by either direct measurements of the unit cell on the HRTEM image or by FFT analysis of the precipitates images [15-18]. Fig. 2 shows a selection of representative types of precipitates from the un-deformed condition. All have various degrees of disorder, but can be classified as follows: disordered β'' (Fig. 2a), disordered β' (Fig. 2b), disordered with Si-network's base plane in $\langle 001 \rangle$ Al where one base vector is along $\langle 100 \rangle$ (Fig. 2c), and undefined disordered (Fig. 2d). It is interesting to notice that the un-deformed condition appears to be a transition stage from β'' to post- β'' precipitates. This is reflected in the images of Fig. 2 which implies that the Si-network itself is distorted

In the presence of grain boundaries only B' precipitates have been found, with larger sizes than the precipitates forming in the matrix.

On the other hand, images of precipitates in the pre-deformed condition indicate that the majority is of post- β'' type, with a more developed crystal structure and a more hexagonal Si-network, see Fig. 3. Many precipitates in this condition which grow along dislocation lines have narrow cross-sections along $\langle 510 \rangle$ Al with ~ 1.04 nm periodicity in this direction only. An example is given in Fig. 3a. In spite of the 1.04 nm periodicity and cross-section elongation, as well as the orientation of the Si network with matrix, which are all characteristics of the hexagonal B' phase, the image does not show

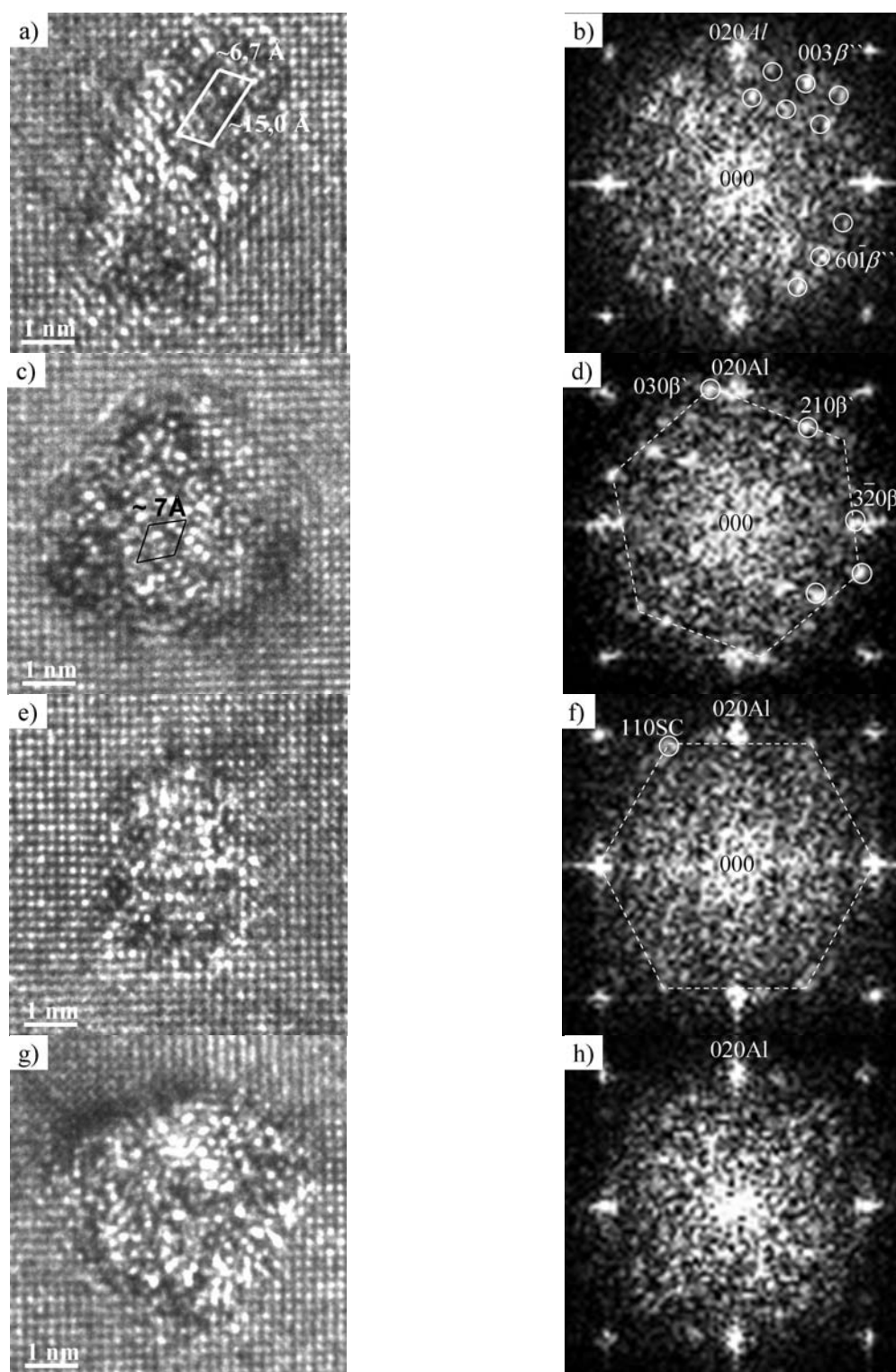


Fig. 2 Precipitate types in the un-deformed AA6060 after 300 min heat treatment at 190°C: (a) Disordered β'' with marked unit cell. (b) FFT of (a) where full circles indicate some spots corresponding to β'' symmetry [13]. (c) Disordered β' with marked unit cell. (d) FFT of (c). Full circles indicate some spots corresponding to β' symmetry [14]. Spots corresponding to the Si-network are connected by dashed lines. (e) Disordered precipitate with Si-network base plane along $\langle 100 \rangle_{Al}$. (f) FFT of (e) where spots corresponding to the Si-network are connected by dashed lines. (g) Undefined disordered precipitate, (h) FFT of (g)

a complete B' unit cell, as is normal for this phase. Based on all available high-magnification images, the numbers and fractions of the precipitates forming during the heat treatment in both conditions have been quantified and the results are presented in Table 3. For both conditions, the precipitate types are divided into β'' and post- β'' . In the pre-deformed material, the post- β'' precipitates could be further divided into several different categories.

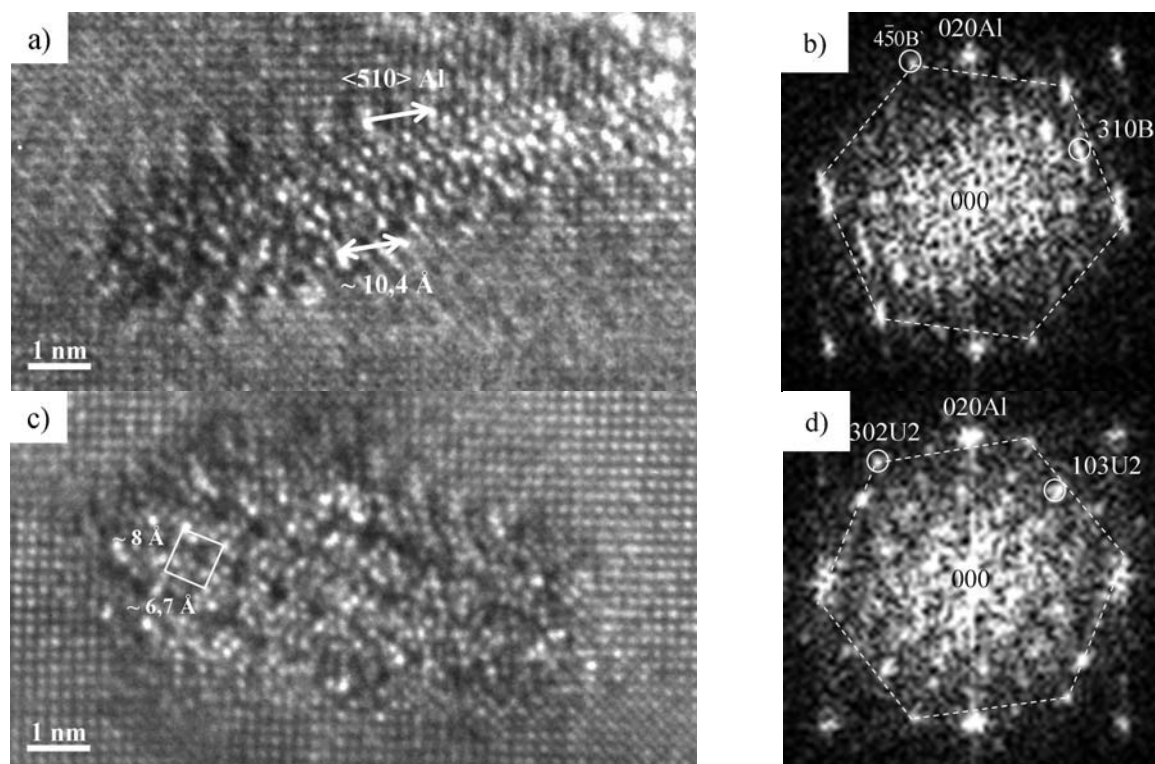


Fig. 3. Precipitate types in AA6060 with 10% pre-deformation after 300 min heat treatment at 190°C: (a) B' like precipitate with the marked periodicity of 10.4 Å along $\langle 510 \rangle_{Al}$. (b) FFT of (a). Full circles indicate some spots corresponding to B' symmetry [15]. Spots corresponding to the Si-network are connected by dashed lines. (c) Disordered U2-precipitate with marked unit cell. (d) FFT of (c). Full circles indicate some spots corresponding to U2 symmetry [16]. Spots corresponding to the Si-network are connected by dashed lines

Table 3. Precipitate statistics for 0% and 10% pre-deformed samples of AA6060 after annealing 300 min at 190°C. The total number of analysed precipitates in the undeformed material was 52, and in the pre-deformed material 59.

Precipitate type [%]	un-deformed	10% pre-deformed
β''	58	3
post- β'' , total	42	97
B'		51
β'		24
U2		3
Unresolved hexagonal		19

Table 3 indicates that the percentage of β'' phase is greatly reduced in the pre-deformed material. Also, the post- β'' precipitates are more developed as compared to the undeformed condition. The results in Table 3 confirm previous observations that more stable precipitates are being formed along dislocation lines in deformed materials [9].

Most of the precipitates in the undeformed material are highly disordered, which makes a determination of the precipitate structure in a lot of cases impossible. The disorder is a result of the transformation from β'' to the post- β'' precipitates, which occurs during this interval. In the deformed material, the precipitates are less disordered. These results show that the precipitation sequence changes in the presence of dislocations. Dislocations serve as heterogeneous nucleation sites, which favour a direct precipitation of post- β'' phases in the pre-deformed material.

4. Conclusion

In the presence of dislocations the precipitation behaviour of the investigated AA6060 alloys changes significantly. The pre-deformed condition produces a lower number density of coarser (longer, thicker) needles with higher volume fraction as compared to the undeformed condition. The preferred nucleation sites in the pre-deformed material are dislocation lines, while in the undeformed material the precipitates are more homogeneously distributed in the Al matrix. The higher volume fraction in the pre-deformed material shows the enhancement of precipitation in the presence of heterogeneous precipitation sites.

Furthermore, determination of precipitate types shows that the presence of dislocations favours the formation of post- β'' precipitates, changing the precipitation sequence from:

GP \rightarrow β'' \rightarrow post β'' -precipitates to: GP \rightarrow post β'' -precipitates

References

- [1] C. D. Marioara, S. J. Andersen, H. W. Zandbergen, R. Holmestad: *Metall. Mat. Trans. A* 36 (2005) 691-702.
- [2] C. D. Marioara, H. Nordmark, S. J. Andersen, R. Holmestad: *J. of Mat. Sci.* 41 (2006)471-478.
- [3] G. A. Edwards and K. Stiller: *Acta Mater.* 46 (1998) 3893-3904.
- [4] K. Matsuda and Y. Sakaguchi: *J. Materials Science* 35 (2000) 179-189.
- [5] S. J. Andersen, C. D. Marioara, R. Vissers, A. G. Frøseth, P. Derlet,: *Proc. of EMC*, 22-27 August 2004, Antwerpen, Belgium, 2, 599-600.
- [6] S. J. Andersen, C. D. Marioara, R. Vissers, A. G. Frøseth, H. W. Zandbergen: *Mat. Sci. Eng. A* 444 (2007) 157-169.
- [7] C. D. Marioara, S. J. Andersen, T. N. Stene, H. Hasting, J. Walmsley, A. T. J. Van Helvoort and R. Holmestad: *Phil. Mag.* 87 (2007) 3385-3413.
- [8] C. Genevois, D. Fabrègue: *Materials Science and Engineering A* 441(2006) 39-48.
- [9] A. Deschamps, F. Livet: *Acta Materialia* 47 (1998) 281-292.
- [10] K. Matsuda, H. Gamada and Y. Uetani: *Journal of Japan Institute of Light Metals* 48 (1998) 471-475.
- [11] K. Matsuda and S. Shimizu: *Journal of the society of materials science japan* 48 (1999) 10-15.
- [12] R. S. Yassar and D. P. Field: *Scripta Materialia* 53 (2005) 299-303.
- [13] M. Kolar, K.O. Pedersen, S. Gulbrandsen-Dahl, T. Bruggemann, and K. Marthinsen (2010). *Materials Science Forum Vols. 638-642* (2010) 261-266.
- [14] M. Kolar, K.O. Pedersen, S. Gulbrandsen-Dahl, K. Teichmann and K. Marthinsen, *ibid.*
- [15] S. J. Andersen, H. W. Zandbergen, J. Jansen, C. Træholt, U. Tundal, O. Reiso: *Acta Mater.* 46 (1998) 3283-3298.
- [16] R. Vissers, M.A. van Huis, J. Jansen, H.W. Zandbergen, C.D. Marioara, S.J. Andersen: *Acta Mater.* 55 (2007) 3815-3823.
- [13] R. Vissers, C. D. Marioara, S. J. Andersen, R. Holmestad: *Aluminium Alloys*, Ed. by J. Hirsch, G. Gottstein, B. Skrotzki (Wiley-VCH, Weinheim 2008) 2, 1263-1269.
- [18] S. J. Andersen, C. D. Marioara, A. G. Frøseth, R. Vissers, H. W. Zandbergen: *Mat. Sci. Eng. A* 390 (2005) 127-138.